Chapter

Analytic and Numerical Results of Bending Deflection of Rectangular Composite Plate

Louay S. Yousuf

Abstract

In this chapter, the derivation of analytic formulation of bending deflection has been done using the theory of classical laminate plate. The method of Navier and Levy solutions are used in the calculation. The composite laminate plate is exposed to out-off plane temperatures and combined loading. The temperature gradient of thermal shock is varied between $60C^{\circ}$ and $-15C^{\circ}$. The combined loading are the bending moment (M_o) in the y-direction and in-plane force (N_{xx}) in the x-direction. The in-plane force (N_{xx}) has a great effect on the bending deflection value within a (95.842%), but the bending moment (M_o) has a small effect on the bending deflection value in the rate of (4.101%). The results are compared and verified for central normal deflection.

Keywords: classical plate theory, composite laminate plate, temperature affect, combined loading

1. Introduction

The effect of temperature and combined loading on composite plate is one of the primary life limiting factors of a bridge engineering application. This chapter will consider the structural evaluation of the localized effect in the bridge engineering. The application of bridge engineering can be found in a structural bridge deck panel. Ray studied the fiber-matrix debonding by applying the thermal shock of thermal fatigue, taking into account the conditioning time. He performed a three-point bending test on glass fiber reinforced with unsaturated polyester and epoxy resin composites in which it exposed to 75 C° of the temperature gradient [1]. Hussein and Alasadi used a numerical analysis of stress and strain values of angle-ply with four-layered symmetric laminated plate under the effect of force resultant (N_{xx}) and bending moment (M_{xx}) graphically. He predicted the material properties of the multilayered plate of the reinforcement fibers of E-glass and epoxy resin [2]. Yousuf et al. evaluated the dynamic analysis of normal deflection, taking into consideration the effect of thermal fatigue beside the effect of bending moment (M_o) and in-plane force (N_{xx}). The composite laminate plate of woven roving fiber glass and polyester were exposed to 75 C° of the temperature gradient. A composite laminate plate with fiber volume fraction $(v_f = 25.076\ \%)$ was selected [3]. Wang et al. applied the thermal cycles in the temperature range between (80 C° and -40 C°) on different plys of glass fiber/epoxy matrix composites. Scanning electron microscopy (SEM) images showed that after 180 of thermal cycles, the bonding effect of glass fiber and epoxy matrix became worse, leading to the decrease in mechanical properties [4].

Khashaba et al. investigated the mechanical properties of $[0]_8$ of woven glass fiber reinforced polyester (GFRP) composites under monotonic and combined tension/bending loading [5, 6]. Yousuf reduced the vibration properties of composite material under the variation of combined temperatures (60 $C°$ to −15 $C°$) using three types of boundary conditions. The free vibration test was carried out for (5, 10, 15, 20, 25, and 30) minutes [7]. Moufari proposed several numerical simulations to describe the interaction between thermal and mechanical stresses. The estimation damage modes of carbon/epoxy laminate plate has been achieved due to thermal cyclic loading. Zhen and Xiaohui proposed an analytic model of Reddy-type higher-order plate theory for simply supported plates based on thermal and mechanical combined loading [8]. In this work, the analytic derivation of bending deflection has been done by using the theory of classical laminate plate. Levy and Navier solutions are used to describe the theory of bending deflection by taking into consideration the use of simply supported boundary condition from all edges. In our point of view, the analytic derivation of normal deflection under the effect of temperature and combined loading has not been studied.

2. Equations of motion in terms of displacements

The stress and strain relationship is varied through the laminate thickness, as indicated in Eq. (1):

$$\begin{bmatrix} \sigma_{xx} \\ \sigma_{yy} \\ \sigma_{xy} \end{bmatrix} = \begin{bmatrix} Q_{11} & Q_{12} & 0 \\ Q_{12} & Q_{22} & 0 \\ 0 & 0 & Q_{66} \end{bmatrix} * \left[\begin{bmatrix} \varepsilon_{xx} \\ \varepsilon_{yy} \\ \gamma_{xy} \end{bmatrix} - \begin{bmatrix} \alpha_1 \\ \alpha_2 \\ 0 \end{bmatrix} * \Delta T \right] \tag{1}$$

The general bending equation of rectangular plate is as below:

$$\frac{\partial^2 M_{xx}}{\partial x^2} + 2\frac{\partial^2 M_{xy}}{\partial x \partial y} + \frac{\partial^2 M_{yy}}{\partial y^2} = 0 \tag{2}$$

By taking into account the temperature effect, the mechanical and thermal bending moments are:

$$\begin{bmatrix} M_{xx} \\ M_{yy} \\ M_{xy} \end{bmatrix} = \begin{bmatrix} M_{xx}^{Mech.} \\ M_{yy}^{Mech.} \\ M_{xy}^{Mech.} \end{bmatrix} - \begin{bmatrix} M_{xx}^{Ther.} \\ M_{yy}^{Ther.} \\ M_{xy}^{Ther.} \end{bmatrix} \tag{3}$$

where

$$\begin{bmatrix} M_{xx}^{Mech.} \\ M_{yy}^{Mech.} \\ M_{xy}^{Mech.} \end{bmatrix} = \begin{bmatrix} B_{11} & B_{12} & 0 \\ B_{12} & B_{22} & 0 \\ 0 & 0 & B_{66} \end{bmatrix} * \begin{bmatrix} \frac{\partial u_o}{\partial x} \\ \frac{\partial v_o}{\partial y} \\ \frac{\partial u_o}{\partial y} + \frac{\partial v_o}{\partial x} \end{bmatrix} - \begin{bmatrix} D_{11} & D_{12} & 0 \\ D_{12} & D_{22} & 0 \\ 0 & 0 & D_{66} \end{bmatrix} * \begin{bmatrix} \frac{\partial^2 w_o}{\partial x^2} \\ \frac{\partial^2 w_o}{\partial y^2} \\ 2\frac{\partial^2 w_o}{\partial x \partial y} \end{bmatrix} \tag{4}$$

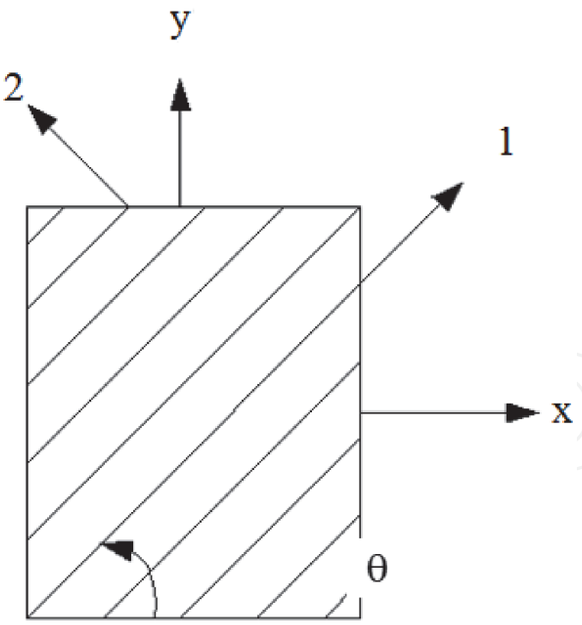

Figure 1.
Lamina of arbitrary of principal material direction.

And,

$$\begin{bmatrix} M_{xx}^{Ther.} \\ M_{yy}^{Ther.} \end{bmatrix} = \sum_{k=1}^{N} \begin{bmatrix} Q_{11} & Q_{12} \\ Q_{12} & Q_{22} \end{bmatrix}^k * \begin{bmatrix} \alpha_1 \\ \alpha_2 \end{bmatrix}^k * \int_{z_k}^{z_{k+1}} \Delta T z dz \tag{5}$$

It can be assumed that all layers have $(\Theta = 0)$, and the same thickness $(B_{ij} = 0)$, as indicated in **Figure 1**. Substitute Eq. (4) and into Eq. (3), it can be obtained:

$$D_{11}\left(\frac{\partial^4 w_o}{\partial x^4}\right) + 2(D_{12} + 2D_{66})\left(\frac{\partial^4 w_o}{\partial x^2 \partial y^2}\right) + D_{22}\left(\frac{\partial^4 w_o}{\partial y^4}\right) + N_{xx}\left(\frac{\partial^2 w_o}{\partial x^2}\right) = -\left(\frac{\partial^2 M_{xx}^{Ther.}}{\partial x^2} + \frac{\partial^2 M_{yy}^{Ther.}}{\partial y^2}\right) \tag{6}$$

3. Formulation of bending deflection distribution using Navier solution

The normal deflection distribution is derived based on the solution of classical laminate plate theory using Navier equation. Navier solution assumed that the boundary condition is simply supported from all edges under the effect of temperature (ΔT) and in-plane force (N_{xx}). It can be assumed that the temperature is varied linearly through the plate thickness, as in below:

$$T_{mn}(z) = \frac{4}{ab}\int_0^a \int_0^b \Delta T(x, y, z)\, sin\,(\alpha_m x)\, sin\,(\beta_n y) dx dy \tag{7}$$

where.

T_1 is the out-off plane uniform temperature when the heat source is applied through the plate thickness.

And,

$$\alpha_m = \frac{m\pi}{a}, m = 1, 2, 3, \ldots, \infty \tag{8a}$$

$$\beta_n = \frac{n\pi}{b}, n = 1, 2, 3, \ldots, \infty \tag{8b}$$

By integrating Eq. (7) with respect to (x) and (y), the temperature distribution through the plate thickness is:

$$T_{mn}(z) = \frac{16T_1 z}{mn\pi^2} \tag{9}$$

The thermal bending moment is defined as in the following:

$$\begin{bmatrix} M_{xx}^{Ther.} \\ M_{yy}^{Ther.} \end{bmatrix} = \sum_{m=1}^{\infty}\sum_{n=1}^{\infty} \begin{bmatrix} M_{mn}^{(1)} \\ M_{mn}^{(2)} \end{bmatrix} sin\,(\alpha_m x)\, sin\,(\beta_n y) \tag{10}$$

where

$$M_{mn}^{(1)} = \sum_{k=1}^{N} \int_{z_k}^{z_{k+1}} (Q_{11}\alpha_1 + Q_{12}\alpha_2) T_{mn}(z) z dz \tag{11a}$$

$$M_{mn}^{(2)} = \sum_{k=1}^{N} \int_{z_k}^{z_{k+1}} (Q_{12}\alpha_1 + Q_{22}\alpha_2) T_{mn}(z) z dz \tag{11b}$$

The general solution of normal deflection for simply supported boundary condition from all edges is:

$$w_o = \sum_{m=1}^{\infty}\sum_{n=1}^{\infty} w_{mn}\, sin\,(\alpha_m x)\, sin\,(\beta_n y) \tag{12}$$

Substitute Eq. (12) and Eq. (10) into Eq. (6), the solution of bending deflection is illustrated in the following equation:

$$w_o(x,y) = \frac{16T_1}{3\pi^2} \sum_{m=1}^{\infty}\sum_{n=1}^{\infty} \frac{\left(A_1\alpha_m^2 + A_2\beta_n^2\right) sin\,(\alpha_m x)\, sin\,(\beta_n y)}{mn\left(D_{11}\alpha_m^4 + 2(D_{12} + 2D_{66})\alpha_m^2\beta_n^2 + D_{22}\beta_n^4 - N_{xx}\alpha_m^2\right)} \tag{13}$$

where

$$A_1 = \sum_{k=1}^{N} (Q_{11}\alpha_1 + Q_{12}\alpha_2)\left(z_{k+1}^3 - z_k^3\right) \tag{14a}$$

$$A_2 = \sum_{k=1}^{N} (Q_{12}\alpha_1 + Q_{22}\alpha_2)\left(z_{k+1}^3 - z_k^3\right) \tag{14b}$$

4. Formulation of bending deflection distribution using levy solution

The theory of classical laminate plate of Levy solution is used to derive the solution of normal deflection. The Levy solution assumed that the variation of the

bending deflection should be along the x-axis. Levy solution can be used on any type of boundary condition which gives flexibility on any type of loading such as (ΔT), in-plane force (N_{xx}), and bending moment (M_o). As mentioned in the previous section that the temperature is varied linearly through the plate thickness, as below:

$$T_m(z) = \frac{2}{a}\int_0^a \Delta T(x,z)\, sin\,(\alpha_m x)dx \tag{15}$$

where

$$\alpha_m = \frac{m\pi}{a}, m = 1, 2, 3, \ldots, \infty \tag{16}$$

By integrating Eq. (15) with respect to (x), the temperature distribution through the plate thickness is:

$$T_m(z) = \frac{4T_1 z}{m\pi} \tag{17}$$

Ignore the variation of thermal bending moment and normal deflection along y-axis, Eq. (6) will be:

$$D_{11}\left(\frac{\partial^4 w_o}{\partial x^4}\right) + N_{xx}\left(\frac{\partial^2 w_o}{\partial x^2}\right) = -\frac{\partial^2 M_{xx}^{Ther.}}{\partial x^2} \tag{18}$$

As mentioned earlier, the thermal bending moment is varied along x-axis, as below:

$$\left[M_{xx}^{Ther.}\right] = \sum_{m=1}^{\infty}\left[M_m^{(1)}\right] sin\,(\alpha_m x) \tag{19}$$

where

$$M_m^{(1)} = \sum_{k=1}^{N}\int_{z_k}^{z_{k+1}} (Q_{11}\alpha_1) T_m(z) z dz \tag{20}$$

The solution of normal bending deflection is as below:

$$w_o(x,y) = w_o(x,y)_H + w_o(x)_P \tag{21}$$

To find $w_o(x)_P$:

$$w_o(x,t)_p = \sum_{m=1}^{\infty} w_m\, sin\,(\alpha_m x) \tag{22}$$

Substitute Eq. (19) and Eq. (22) into Eq. (18) to obtain the particular solution of bending deflection along x-axis, $w_o(x)_P$:

$$w_o(x)_p = \frac{4T_1 A_1}{3\pi}\sum_{m=1}^{\infty}\frac{\alpha_m^2\, sin\,(\alpha_m x)}{m\left(D_{11}\alpha_m^4 - N_{xx}\alpha_m^2\right)} \tag{23}$$

where

$$A_1 = \sum_{k=1}^{N} (Q_{11}\alpha_1)\left(z_{k+1}^3 - z_k^3\right) \tag{24}$$

To find $w_o(x,y)_H$, Eq. (6) will be:

$$D_{11}\frac{\partial^4 w_o}{\partial x^4} + 2(D_{12} + 2D_{66})\frac{\partial^4 w_o}{\partial x^2 \partial y^2} + D_{22}\frac{\partial^4 w_o}{\partial y^4} + N_{xx}\frac{\partial^2 w_o}{\partial x^2} = 0 \tag{25}$$

The solution of Eq. (25) is as below:

$$w_o(x,y)_H = \sum_{m=1}^{\infty} Y_m \sin(\alpha_m x) \tag{26}$$

Substitute Eq. (26) into Eq. (25), to obtain the homogeneous solution of Eq. (25) along x- and y-directions:

$$w_o(x,y)_H = \sum_{m=1}^{\infty} [N_1 \cosh(\alpha y) + N_2 \sinh(\alpha y) + N_3 \cos(\beta y) + N_4 \sin(\beta y)] \sin(\alpha_m x) \tag{27}$$

Substitute Eq. (27) and Eq. (23) into Eq. (21) to obtain the general solution of normal bending deflection, as indicated below:

$$w_o(x,y) = \sum_{m=1}^{\infty} [N_1 \cosh(\alpha y) + N_2 \sinh(\alpha y) + N_3 \cos(\beta y) + N_4 \sin(\beta y)] \sin(\alpha_m x) + \frac{4T_1 A_1}{3\pi} \sum_{m=1}^{\infty} \frac{\alpha_m^2 \sin(\alpha_m x)}{m\left[D_{11}\alpha_m^4 - N_{xx}\alpha_m^2\right]} \tag{28}$$

The simply supported boundary conditions from all edges are assumed and the constants $(N_1, N_2, N_3, and\ N_4)$ are as below:

$$N_1 = -\frac{\beta^2 H}{\left(\alpha^2 + \beta^2\right)} - \frac{4M_o}{\left(\alpha^2 + \beta^2\right)m\pi D_{22}} \tag{29}$$

$$N_2 = \frac{\cosh(\alpha b)\beta^2 H}{\left(\alpha^2 + \beta^2\right)\sinh(\alpha b)} + \frac{4\cosh(\alpha b)M_o}{\left(\alpha^2 + \beta^2\right)\sinh(\alpha b)m\pi D_{22}} - \frac{\left(D_{12}\alpha_m^2 + \beta^2 D_{22}\right)H}{\left(\alpha^2 + \beta^2\right)\sinh(\alpha b)D_{22}} - \frac{\left(\frac{4M_o}{m\pi} - D_{12}\alpha_m^2 H\right)}{\left(\alpha^2 + \beta^2\right)\sinh(\alpha b)D_{22}} \tag{30}$$

$$N_3 = -\frac{\alpha^2 H}{\left(\alpha^2 + \beta^2\right)} + \frac{4M_o}{\left(\alpha^2 + \beta^2\right)m\pi D_{22}} \tag{31}$$

$$N_4 = \frac{\cos(\beta b)\alpha^2 H}{\left(\alpha^2 + \beta^2\right)\sin(\beta b)} - \frac{4\cos(\beta b)M_o}{\left(\alpha^2 + \beta^2\right)\sin(\beta b)m\pi D_{22}} - \frac{\left(\alpha^2 D_{22} - D_{12}\alpha_m^2\right)H}{\left(\alpha^2 + \beta^2\right)D_{22}\sin(\beta b)} + \frac{\left(\frac{4M_o}{m\pi} - D_{12}\alpha_m^2 H\right)}{\left(\alpha^2 + \beta^2\right)\sin(\beta b)D_{22}} \tag{32}$$

where

$$H = \frac{4T_1A_1\alpha_m^2}{3\pi m\left(D_{11}\alpha_m^4 - N_{xx}\alpha_m^2\right)} \tag{33}$$

5. Numerical simulation procedure

In this chapter, the finite element discretization is carried out by using ANSYS Ver. 18.2. (SHELL 132) element is used to mesh the composite laminate plate. SHELL 132 is defined by eight nodes having six degrees of freedom at each node to calculate the central normal deflection. In the simulation analysis, the central point of laminate plate is used to calculate the normal deflection. Always the convergence test is needed to determine the size of elements in which the value of normal bending deflection settles down. Finite element analysis of convergence curve defines the relationship between the grid interval and the analysis accuracy. Four types of combined loading is used such as: (temperature affect only (ΔT)), (temperature affect (ΔT) + Mo), (temperature affect (ΔT) + Nxx), and (temperature affect (ΔT) + Mo + Nxx). Multiple values of fiber volume fraction is used such as (25, 40, 50, 60, 70, and 80)%. **Table 1** shows the mechanical and thermal properties of the simulated materials.

ν_f	**25.07%**	**40%**	**50%**	**60%**	**70%**	**80%**
$E_x^c(GPa.)$	19.933	30.4038	37.41988	44.435	51.452	58.468
$E_y^c(GPa.)$	19.933	30.4038	37.41988	44.435	51.452	58.468
$E_z^c(GPa.)$	3.0896	3.81746	4.53322	5.5793	7.25302	10.3612
ν_{12}	0.3835	0.35098	0.32915	0.30732	0.2855	0.26366
$G_{12}(GPa.)$	1.07675	1.33379	1.5878	1.9614	2.5648	3.70468
$\rho_c(kg/m^3)$	1464.18	1686.48	1835.4	1984.32	2133.24	2282.16
$\alpha_x^c(1/C^\circ)$	25.746 E-6	21.6044 E-6	18.5098 E-6	15.3005 E-6	12.0234 E-6	8.70307 E-6
$\alpha_y^c(1/C^\circ)$	25.746 E-6	21.6044 E-6	18.5098 E-6	15.3005 E-6	12.0234 E-6	8.70307 E-6
$\alpha_z^c(1/C^\circ)$	10.5844 E-6	7.932 E-6	6.9852 E-6	6.3374 E-6	5.8663 E-6	5.5082 E-6
$k_x^c(W/mC^\circ)$	0.4533	0.622	0.735	0.848	0.961	1.074
$k_y^c(W/mC^\circ)$	0.4533	0.622	0.735	0.848	0.961	1.074
$k_z^c(W/mC^\circ)$	0.2174	0.2626	0.30068	0.3553	0.43418	0.55808
$C_p^c(J/kgC^\circ)$	768.139	780.8944	787.7133	793.5087	798.495	802.8304

Table 1.
Mechanical and thermal properties of the simulated materials.

6. Results and discussions

Figures 2 and **3** show the verification test of normal bending deflection using Levy and Navier solutions, taking into consideration ANSYS 18.2 results. The normal bending deflection decreased with the increasing of plate aspect ratio because of the increasing in plate bending stiffness under the temperature effect $(60C^\circ)$ and $(-15C^\circ)$ for fiber volume fraction (25.076%). The bending deflection value when

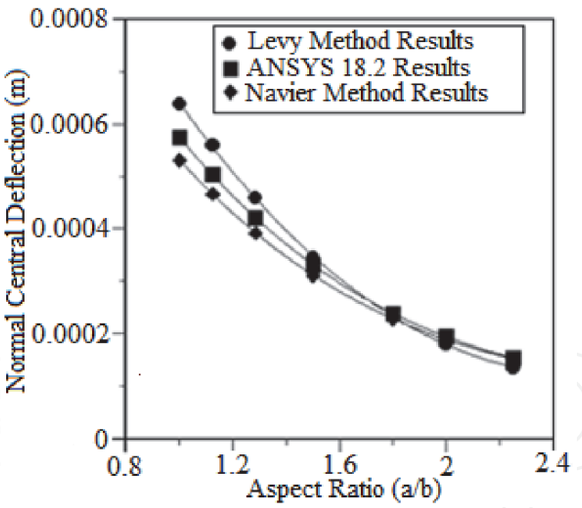

Figure 2.
Normal bending deflection varying with laminate plate aspect ratio under temperature effect $(60C^{\circ})$.

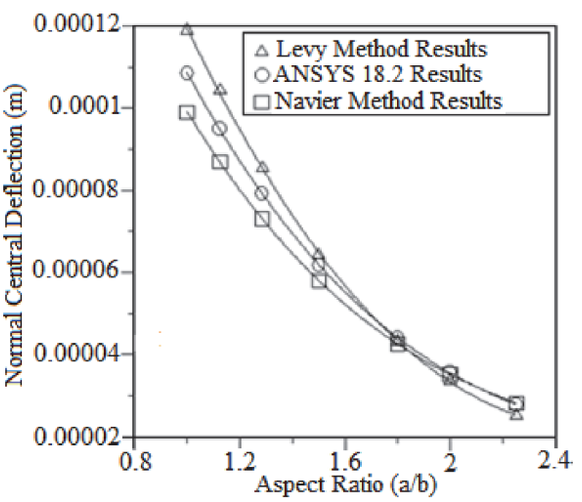

Figure 3.
Normal bending deflection varying with laminate plate aspect ratio under temperature effect $(-15C^{\circ})$.

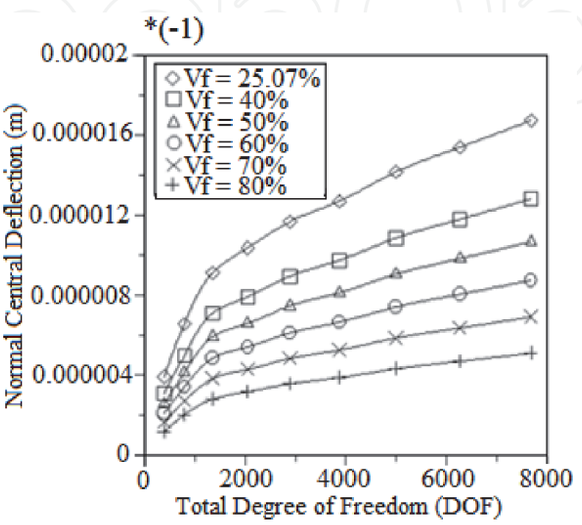

Figure 4.
Convergence test of normal deflection and total degrees of freedom under the effect of temperature (ΔT)*, bending moment* (M_o)*, and in-plane force* (N_{xx}).

Deflection	Levy method results	ANSYS 18.2 results	Percentage error (%)
(ΔT)	0.1853e-3	0.1880e-3	1.748
(ΔT)+ (M_o)	−0.1777e-3	−0.1882e-3	5.536
(ΔT)+ (N_{xx})	0.7704e-5	0.7108 e-5	7.736
(ΔT)+ (M_o)+(N_{xx})	−0.9859e-5	−0.9365e-5	5.010

Table 2.
Analytic and simulation verification of bending deflection under combined loading.

$(T = 60C^{\circ})$ is higher than the value of bending deflection when $(T = -15C^{\circ})$ because of the expansion and contraction through the plate laminate thickness.

Figure 4 shows the convergence test of normal bending deflection with total degrees of freedom for different fiber volume fractions using ANSYS software. The normal central deflection decrease with the increasing of fiber volume fraction under the effect of temperature (ΔT), bending moment (M_o), and in-plane force (N_{xx}).

Table 2 shows the analytic and simulation verification results of bending deflection under combined loadings for fiber volume fraction $v_f = 25.076\%$ and plate aspect ratio (1.8). The value of central deflection of the system with combined loading (ΔT) is higher than the others of combined loading. The deflection of system with combined loading $(\Delta T + M_o + N_{xx})$ and the system with loading $(\Delta T + N_{xx})$ is almost the same and in the opposite direction because bending moment has a small effect.

7. Conclusions

As mentioned in Introduction section, Levy and Navier solutions are used to describe the theory of bending deflection by taking into consideration the use of simply supported boundary condition from all edges. ANSYS software is used in the convergence test. The bending deflection value when $(T = 60C^{\circ})$ is higher than the value of bending deflection when $(T = -15C^{\circ})$ because of the expansion and contraction through the plate laminate thickness. The in-plane force (N_{xx}) has a great effect on the bending deflection value of composite laminate plate, but the bending moment (M_o) has a small effect on the bending deflection value. The normal deflection is decreased with the increasing of fiber volume fraction from 25.07% to 80% under the effect of (ΔT) and combined loading (M_o) + (N_{xx}). Moreover, the normal bending deflection is decreased with the increasing of aspect ratio from 0.8 to 2.4 under the effect of $(T = 60C^{\circ})$ and $(T = -15C^{\circ})$, respectively.

Nomenclature

α_1, α_2	thermal expansion coefficient in longitudinal and lateral directions, $1/C^{\circ}$.
ΔT	gradient uniform temperature, C°.
A_1, A_2	bending moment due to temperature, N.m/C°.
M_{xx}, M_{yy}, and M_{xy}	bending and twist moments, N.m.
Q_{ij}	reduced stiffness elements, N/m^2.
w_0	midplane deflection along z-direction.
z_k, z_{k+1}	upper and lower lamina surface coordinates along z-direction, m.

a, b	length of large and small spans of rectangular plate (m).
m, n	double trigonometric of Furrier series.
N	total number of layers.

Author details

Louay S. Yousuf
Department of Mechanical Engineering, San Diego State University, San Diego, CA, USA

*Address all correspondence to: louaysabah79@yahoo.com

References

[1] Ray B. Thermal shock and thermal fatigue on delamination of glass-fiber-reinforced polymeric composites. Journal of Reinforced Plastics and Composites. 2005;**24**(1):111-116

[2] Hussein EQ, Alasadi SJ. Experimental and theoretical stress analysis for composite plate under combined load. Journal of University of Babylon. Babylon University; 2018;**26**(1):129-140

[3] Yousuf LS, Jameel AN, AL-Sahib NKA. Verification of laminate composite plate simulation under combined loadings thermal stresses. Journal of Engineering. 2010;**16**(4):6123-6142

[4] Wang D, Zhou X, Ge H, Liu Z, Liu H, Sun K. The influence of thermal fatigue on the properties of glass fiber/epoxy composites. Polymers & Polymer Composites. 2012;**20**(1-2):129-132

[5] Khashaba U, Aldousari S, Najjar I. Behavior of $[0]_8$ woven composites under combined bending and tension loading: Part-i experimental and analytical. Journal of Composite Materials. 2012;**46**(11):1345-1355

[6] Onyechi PC, Asiegbu KO, Chinenye AL. Effect of volume fraction on the mechanical properties of Periwinkle shell reinforced polyester composite (PRPC). American Journal of Mechanical Engineering and Automation. Open Science Publisher; 2015;**2**(1):1-15

[7] Yousuf LS. Time prediction of dynamic behavior of glass fiber reinforced polyester composites subjected to fluctuating varied temperatures. Al-Khwarizmi Engineering Journal. 2018;**5**(3):28-37

[8] Zhen W, Xiaohui R. Thermomechanical analysis of multilayered plates in terms of Reddy-type higher-order theory. Journal of Advanced Materials and Structures. Taylor & Francis Publisher; 2017;**24**(14):1196-1205